(2)

DNA-TR-88-140

APPROXIMATIONS OF SURFACE ROUGHNESS EFFECTS FOR AIRBLAST CALCULATIONS

T. H. Pierce
S-CUBED
A Division of Maxwell Laboratories, Inc.
P.O. Box 1620
La Jolla, CA 92038-1620

1 November 1985

Technical Report

CONTRACT No. DNA 001-85-C-0024

THIS WORK WAS SPONSORED BY THE DEFENSE NUCLEAR AGENCY
UNDER RDT&E RMC CODE B344085466 RS RA 00046 25904D.

Prepared for
Director
Defense Nuclear Agency
Washington, DC 20305-1000

Destroy this report when it is no longer needed. Do not return to sender.

PLEASE NOTIFY THE DEFENSE NUCLEAR AGENCY ATTN: TITL, WASHINGTON, DC 20305 1000, IF YOUR ADDRESS IS INCORRECT, IF YOU WISH IT DELETED FROM THE DISTRIBUTION LIST, OR IF THE ADDRESSEE IS NO LONGER EMPLOYED BY YOUR ORGANIZATION.

DISTRIBUTION LIST UPDATE

This mailer is provided to enable DNA to maintain current distribution lists for reports. We would appreciate your providing the requested information.

☐ Add the individual listed to your distribution list.

☐ Delete the cited organization/individual.

☐ Change of address.

NAME: _____

ORGANIZATION: _____

OLD ADDRESS	CURRENT ADDRESS
_____	_____
_____	_____
_____	_____

TELEPHONE NUMBER: ( ) _____

SUBJECT AREA(s) OF INTEREST:

_____	_____
_____	_____
_____	_____

DNA OR OTHER GOVERNMENT CONTRACT NUMBER: _____

CERTIFICATION OF NEED-TO-KNOW BY GOVERNMENT SPONSOR (if other than DNA):

SPONSORING ORGANIZATION: _____

CONTRACTING OFFICER OR REPRESENTATIVE: _____

SIGNATURE: _____

CUT HERE AND RETURN

Director
Defense Nuclear Agency
ATTN: TITL
Washington, DC 20305-1000

Director
Defense Nuclear Agency
ATTN: TITL
Washington, DC 20305-1000

REPORT DOCUMENTATION PAGE

1a REPORT SECURITY CLASSIFICATION UNCLASSIFIED	1b RESTRICTIVE MARKINGS
2a SECURITY CLASSIFICATION AUTHORITY N/A since unclassified	3 DISTRIBUTION/AVAILABILITY OF REPORT Approved for public release; distribution is unlimited.
2b DECLASSIFICATION/DOWNGRADING SCHEDULE N/A since unclassified	
4 PERFORMING ORGANIZATION REPORT NUMBER(S) SSS-R-86-7600/R1	5 MONITORING ORGANIZATION REPORT NUMBER(S) DNA-TR-88-140
6a NAME OF PERFORMING ORGANIZATION S-CUBED, A Division of Maxwell Laboratories, Inc. 6b OFFICE SYMBOL (If applicable)	7a NAME OF MONITORING ORGANIZATION Director Defense Nuclear Agency
6c ADDRESS (City, State, and ZIP Code) P.O. Box 1620 La Jolla, CA 92038-1620	7b ADDRESS (City, State, and ZIP Code) Washington, DC 20305-1000
8a NAME OF FUNDING/SPONSORING ORGANIZATION 8b OFFICE SYMBOL (If applicable) SPWE/Wade	9 PROCUREMENT INSTRUMENT IDENTIFICATION NUMBER DNA 001-85-C-0024
8c ADDRESS (City, State, and ZIP Code)	10 SOURCE OF FUNDING NUMBERS PROGRAM ELEMENT NO: 62715H; PROJECT NO: RS; TASK NO: RA; WORK UNIT ACCESSION NO: DH008681

11 TITLE (Include Security Classification)
APPROXIMATIONS OF SURFACE ROUGHNESS EFFECTS FOR AIRBLAST CALCULATIONS

12 PERSONAL AUTHOR(S)
Pierce, T. H.

13a TYPE OF REPORT	13b TIME COVERED	14 DATE OF REPORT (Year, Month, Day)	15 PAGE COUNT
Technical	FROM 850701 TO 851015	851101	24

16 SUPPLEMENTARY NOTATION
This work was sponsored by the Defense Nuclear Agency under RDT&E RMC Code B344085466 RS RA 00046 25904D.

17 COSATI CODES			18 SUBJECT TERMS (Continue on reverse if necessary and identify by block number)
FIELD	GROUP	SUB-GROUP	
20	04		Roughness, Jet flow, Boundary Layer, surface shear, Non-ideal Airblast, TURBULENT Boundary Layer (JES)
20	11		

19 ABSTRACT (Continue on reverse if necessary and identify by block number)

A brief description of roughness effects on a boundary layer is given. The effects of the amount of areal roughness coverage on the law of the wall are summarized. The concept of hydrodynamically equivalent rough surfaces is discussed. The issue of non-uniform roughness element size is addressed. Some comments are offered relative to roughness scaling.

20 DISTRIBUTION/AVAILABILITY OF ABSTRACT ☐ UNCLASSIFIED/UNLIMITED ☒ SAME AS RPT ☐ DTIC USERS	21 ABSTRACT SECURITY CLASSIFICATION UNCLASSIFIED
22a NAME OF RESPONSIBLE INDIVIDUAL Sandra E. Young	22b TELEPHONE (Include Area Code) (202) 325-7042 22c OFFICE SYMBOL DNA/CSTI

DD FORM 1473, 84 MAR 83 APR edition may be used until exhausted. All other editions are obsolete.

CONVERSION TABLE

Conversion factors for U.S. Customary to metric (SI) units of measurement

MULTIPLY TO GET	BY	TO GET DIVIDE
angstrom	1.000 000 X E -10	meters (m)
atmosphere (normal)	1 013 25 X E +2	kilo pascal (kPa)
bar	1 000 000 X E +2	kilo pascal (kPa)
barn	1 000 000 X E -28	meter^2 (m^2)
British thermal unit (thermochemical)	1.054 350 X E +3	joule (J)
calorie (thermochemical)	4 184 000	joule (J)
cal (thermochemical)/cm^2	4 184 000 X E -2	mega joule/m^2 (MJ/m^2)
curie	3 700 000 X E +1	*giga becquerel (GBq)
degree (angle)	1 745 329 X E -2	radian (rad)
degree Fahrenheit	$t_k = (t°f + 459\ 67)/1.8$	degree kelvin (K)
electron volt	1.602 19 X E -19	joule (J)
erg	1 000 000 X E -7	joule (J)
erg/second	1.000 000 X E -7	watt (W)
foot	3 048 000 X E -1	meter (m)
foot-pound-force	1.355 818	joule (J)
gallon (U S liquid)	3 785 412 X E -3	meter^3 (m^3)
inch	2 540 000 X E -2	meter (m)
jerk	1 000 000 X E +9	joule (J)
joule/kilogram (J/kg) (radiation dose absorbed)	1.000 000	Gray (Gy)
kilotons	4 183	terajoules
kip (1000 lbf)	4 448 222 X E +3	newton (N)
kip/inch^2 (ksi)	6 894 757 X E +3	kilo pascal (kPa)
ktap	1 000 000 X E +2	newton-second/m^2 (N-s/m^2)
micron	1 000 000 X E -6	meter (m)
mil	2 540 000 X E -5	meter (m)
mile (international)	1.609 344 X E +3	meter (m)
ounce	2 834 952 X E -2	kilogram (kg)
pound-force (lbs avoirdupois)	4.448 222	newton (N)
pound-force inch	1 129 948 X E -1	newton-meter (N·m)
pound-force/inch	1 751 268 X E +2	newton/meter (N/m)
pound-force/foot^2	4.788 026 X E -2	kilo pascal (kPa)
pound-force/inch^2 (psi)	6 894 757	kilo pascal (kPa)
pound-mass (lbm avoirdupois)	4 535 924 X E -1	kilogram (kg)
pound-mass-foot^2 (moment of inertia)	4 214 011 X E -2	kilogram-meter^2 (kg·m^2)
pound-mass/foot^3	1 601 846 X E +1	kilogram/meter^3 (kg/m^3)
rad (radiation dose absorbed)	1.000 000 X E -2	**Gray (Gy)
roentgen	2 579 760 X E -4	coulomb/kilogram (C/kg)
shake	1 000 000 X E -8	second (s)
slug	1.459 390 X E +1	kilogram (kg)
torr (mm Hg, 0° C)	1.333 22 X E -1	kilo pascal (kPa)

*The becquerel (Bq) is the SI unit of radioactivity, 1 Bq = 1 event/s
**The Gray (Gy) is the SI unit of absorbed radiation

TABLE OF CONTENTS

SECTION 1
INTRODUCTION

Recent computational experience has indicated that flow interactions with a surface can materially alter precursor structure formation in a non-ideal airblast. The near-surface precursor flow includes a "jet" that interacts with and exchanges momentum with the surface boundary layer. The transition between the off-surface jet flow and the flow in the boundary layer is smooth; the demarcation between the two regions is indistinct. Momentum lost to the ground through surface shear is diffused by turbulence through the boundary layer into the jet without interruption. The jet velocity is reduced and the jet pressure increased due to this effect. The rate at which work is transmitted to the precursor toe is diminished, resulting in a reduction in the overall precursor length.

The detailed character of the surface affects both the extent of airflow momentum loss and the concomitant turbulent diffusivity within the boundary flow. The collective surface conditions that control these effects establish its "roughness". Four properties of the surface appear to have first-order effects. These are: (1) the type of surface irregularities (depressions or protuberances), (2) the size of the irregularities, (3) the fractional amount of surface covered by irregularities, and (4) the geometry of the irregularities.

The effects of depression type (d-type) roughness differ somewhat from those of protuberance-type (k-type) roughness (Reference 1). However, d-type roughness is considered to be of lesser immediate interest and will not be considered further in this discussion.

The contributions to surface roughness arise predominantly from fixed surface protrusions. In desert terrains, fixed surface protrusions may include shrubs, trees, rocks, and ground clods. Loose, lightweight material such as non-fixed pebbles, vegetative debris, and dust cannot support significant shear. These materials

tend to be lofted into the boundary layer and diffused upward by turbulence. Momentum is exchanged between lofted material and the air, but there is essentially no loss of momentum to the ground, as with fixed protrusions.

A real surface may comprise an essentially continuous distribution of protrusion heights. Nevertheless, it is useful to discuss the isolated effects of groups of these protrusions possessing grossly equivalent geometry and size. In such groups, individual members are referred to as "roughness elements". Typical, simplified roughness element models include surface-attached spheres, hemispheres, cones, and cylinders.

Elements that are shorter than a specific minimum vertical size, dependent only on flow conditions, do not contribute measurably to roughness effects. If all roughness elements on a given surface fall below this height, the surface is said to be "hydraulically smooth".

The steady-state, clean-flow (no dust), turbulent boundary layer of a flow over a hydraulically smooth surface consists of four distinctive regions. The innermost of these regions contacts the surface and extends vertically to about 0.1% of the overall boundary-layer thickness. The flow in this "sublayer" is essentially laminar and the velocity increases linearly with height from zero at the surface. Turbulence kinetic energy grows rapidly above the laminar sublayer in a second region referred to as the "buffer" layer. This growth levels off at about 1-2% of the boundary layer thickness, which marks the beginning of the third, "log-law" layer. The turbulence energy is nearly constant throughout the log-law region which extends to about 10% of the boundary layer thickness. Flow conditions in the log-law region are well behaved. Turbulence production and dissipation are in a state of near equilibrium which is reflected by a relatively slow variation in turbulence kinetic energy. The velocity increases logarithmically with height.

The laminar sublayer and buffer layer taken together are often referred to as the "viscous sublayer". The viscous sublayer and the log-law region together comprise the "inner layer" of the boundary layer flow. The remaining 90% of the boundary layer comprises the "outer region". In simple flat-plate flow, turbulence energy drops off in the outer region while the turbulence length scale increases.

The four-layer smooth-wall boundary flow structure begins to be disrupted when surface roughness elements protrude above the laminar sublayer into the buffer region. The extent of this disruption increases with further increases in roughness element size. Turbulence near the surface is enhanced and small turbulent eddies penetrate into the laminar sublayer. When the roughness elements are large enough as to extend into the log-law region, a viscous sublayer is completely absent. The inner layer then consists only of a log-law region, and the surface is said to be "fully rough".

A criterion widely used to distinguish a hydraulically smooth surface is

$$y_R \lesssim 5 \frac{\nu}{u_\tau} \quad , \tag{1}$$

where y_R is the roughness element height, ν is the kinematic viscosity of the flow, and u_τ is the "shear" or "friction" velocity, $u_\tau \equiv (\tau_w/\rho_w)^{1/2}$ (in which τ_w is the surface shear stress and ρ_w is the fluid density at the wall). On the other hand, the surface can be considered fully rough when

$$y_R \gtrsim 70 \frac{\nu}{u_\tau} \quad . \tag{2}$$

These criteria cannot easily be applied, unfortunately, unless an estimate (or measurement) of the surface shear is available. For some purposes, a satisfactory estimate for this purpose can be taken by reference to an approximately comparable flat plate flow. In a simple incompressible flow over a flat plate, the skin friction coefficient, $C_f = \tau_w/(0.5\rho u_E^2)$ can be found from the Schoenherr formula,

$$C_f^{1/2}\left[1.80\ \ell n\left(Re_x C_f\right) + 1.7\right] = 1 \ , \qquad (3)$$

where Re_x is the Reynolds number based on the distance from the leading edge of the plate, $Re_x = u_E X/\nu$, and u_E is the velocity external to the boundary layer. A useful direct relation between u_τ and C_f is

$$\frac{u_\tau}{u_E} = (C_f/2)^{1/2} \ . \qquad (4)$$

SECTION 2
EFFECT OF AREAL COVERAGE

The remainder of the present discussion will consider only the fully rough condition. For this case, the velocity profile of a simple, incompressible, non-separating boundary layer, up to about 10% of the boundary layer thickness, is well represented by the rough-wall Clauser "wall function",

$$\frac{u}{u_\tau} = \frac{1}{\kappa} \ell n\left(\frac{y}{y_R}\right) + C' \quad . \tag{5}$$

Here $\kappa = 0.41$ (Von Karman's constant) is fixed and universal, but the value of C' varies with the roughness element geometry and area coverage.

Figure 1 is a plot of C' as a function of fractional area coverage,

$$f_R \equiv A_R/A \quad , \tag{6}$$

where A_R is the horizontal projected surface area covered by roughness within area A. Data points on this figure were derived from Reference 2. The data points shown individually on this plot are for three-dimensional roughness elements as opposed to two-dimensional elements such as transverse rods.

Smaller values of C' reflect greater ground shear on surfaces having roughness elements of equal height y_R. This is true regardless of changes in the geometry of the elements, if the exterior flowfield is held fixed. The data for spherical roughness elements show that C' is not a monotonic function of f_R. A minimum occurs at 20-25% (depending on which curvefit is used). The data for other three-dimensional roughness elements is insufficient on Figure 1 to exhibit a minimum. However, the curvefit by Dvorak (Reference 3), which was fit through data for both two- and three-dimensional roughness

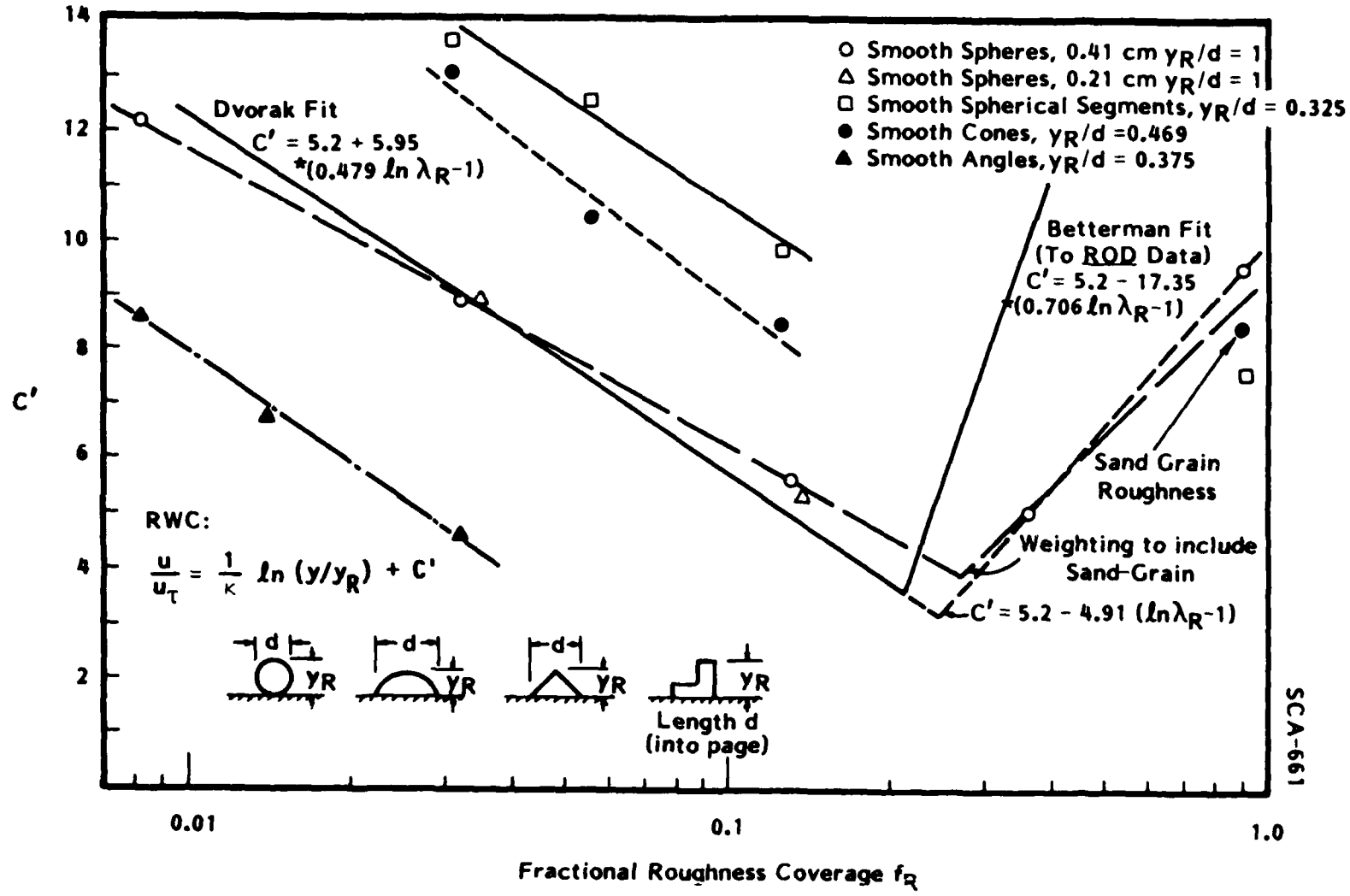

Figure 1. Clauser Log-Law constant C′ vs. fractional roughness coverage, $f_R = A_R/A$. (A_R = area covered by roughness, A = total area; $\lambda_R \equiv 1/f_R$ is "roughness density").

elements, and that by Betterman (Reference 4) for strictly two-dimensional elements are also shown on the figure. The collective data to which these curves were fit suggest that a minimum value of C' exists for all roughness geometries, but that the value of the minimum may change according to the geometry.

The drag on a single roughness element is a function of its vertical projected area, or "lateral area", A_L, while the amount of surface covered by one element is a function of its horizontal projected area, A_R'. For example, a vertical cylinder of diameter d and height h has a lateral area of $A_L = dh$ and a specific surface area of $A_R' = \pi d^2/4$. It is not surprising that the values of C' are smaller for those roughness element geometries which have larger values of A_L/A_R'. For the surface-tangent spheres on Figure 1, $A_L/A_R' = 1$. By comparison, the conical elements ($y_R/d = 0.469$) have $A_L/A_R' = 0.299$, and the angles (neglecting their horizontal part, and assuming the thickness of the vertical part to be d/5), have $A_L/A_R' = 1.88$.

As the number of roughness elements per unit area (that is, the fractional coverage) increases, the drag coefficient associated with the individual elements initially remains constant. However, when the spacing between elements is reduced to several element heights, flow interactions between elements cause the velocity in their vicinity to decrease. The drag coefficient based on the exterior flow velocity then abruptly falls off. This effect has been investigated in some detail by Marshall (Reference 5), and helps to explain the characteristic shape of the C' vs. f_R curves in Figure 1. When f_R is small, the drag coefficient of individual elements is at its highest level and does not change appreciably with moderate increases in f_R. Hence a larger number of roughness elements simply transmits a larger total force to the surface. This is reflected by a steady decrease in C' with increasing f_R. Above the coverage at which the element drag coefficient begins to decline, increases in the number of elements is offset by decreases in the drag per element. The total force transmitted to the surface drops off with further increases in f_R, and the value of C' increases.

It is of interest to note that in Marshall's experiments, only the amount of coverage and not the distribution of roughness elements on the surface appeared to influence the results. That is, regular arrays and randomly distributed elements produced equivalent effects in these experiments. Most of the tests were carried out with cylindrical roughness elements of varying A_L/A_R (varying d/h), although some experiments were conducted with hemispheres. Another qualification to note is that Marshall's tests, in common with all other experiments referenced in this paper,were carried out in the low subsonic regime.

SECTION 3
EQUIVALENT SURFACE ROUGHNESS

Due to the character of the C' vs. f_R (and geometry) curves, the relative roughness effects of different surfaces cannot be compared in terms of a single, directly measurable quantity. A classical basis for comparison is in terms of "equivalent sand-grain roughness size", K_s. This is the diameter of fixed sand-like elements, packed on a surface such that $f_{Rs} = 0.91$ (and $C' = 8.5$), which would yield the same wall shear as that on a specimen surface with a particular roughness element geometry, height, and coverage. If the value of K_s is known for the specimen surface, the Clauser wall function, Eqn.(5), would be written as

$$\frac{u}{u_\tau} = \frac{1}{\kappa} \ell n\left(\frac{y}{K_s}\right) + 8.5 \quad . \tag{7}$$

In this way, K_s becomes a measure of "roughness scale".

An alternative, equivalent procedure is to rewrite Eqn. (5) in the form

$$\frac{u}{u_\tau} = \frac{1}{\kappa} \ell n\left(\frac{y}{Z_o}\right) \quad , \tag{8}$$

where roughness scale Z_o is related to C' and y_R through

$$Z_o = y_R \, EXP \, (-\kappa C') \quad . \tag{9}$$

Both Eqn. (7) and Eqn. (8) appear in the literature.

Surfaces with equal values of K_s or with equal values of Z_o are hydrodynamically equivalent in terms of roughness effects. Choosing Eqn. (8) as the basis for present comparisons, the Dvorak fit, along with the two-point fit on Figure 1 (for surface-tangent spheres, above $f_R = 0.247$), becomes

$$Z_o = \begin{cases} 1.36 \; y_R f_R^{1.17} & , \; f_R \leq 0.247 \\ 0.0158 \; y_R f_R^{-2.01} & , \; f_R > 0.247 \end{cases} \quad . \tag{10}$$

For example, the value of C′ for a surface covered by 2 cm. dia. rocks (y_R = 2 cm) over 21% of the surface area (f_R = 0.21), is C′ =3.65. The value of C′ for a terrain covered by 100 cm dia., dense spherical shrubs (y_R = 100 cm) over 0.74% of the surface area (f_R = 0.0074) is C′ = 6.67. Both of these conditions correspond to Z_o = 0.438 cm in Eqn. (8). In terms of hydrodynamic roughness effects, the two surfaces are equivalent.

The example cited is significant because it illustrates that a terrain in which the surface appears to be relatively smooth but is vegetated with small, dense shrubs scattered over about 1% of the ground area is hydrodynamically as rough as if the surface were "heavily covered" with rocks. The separation between 2 cm dia. spherical "rocks", corresponding to an areal surface coverage of 21%, is only about 4.2 cm in a uniform hexagonal array.

In order to characterize a surface for boundary layer calculations, only the value of Z_o (or K_s) is needed. However, Eqn (10) applies approximately only for spherical roughness elements and then only at relatively low Mach and Reynolds numbers. It appears that the effects of higher flow speeds on the values of Z_o have not been investigated experimentally. Flow regime effects seem almost certain to influence Z_o through the impact of Mach and Reynolds numbers on the drag coefficients of individual roughness elements. Without detailed experimental or calculated information of this kind, it is difficult to estimate appropriate values for Z_o from field measurements, in a given terrain, of y_R, f_R and roughness element geometry.

SECTION 4
DISTRIBUTED ROUGHNESS SIZES

An additional complication arises when roughness elements of different sizes and geometries are present. This is, of course, the case for all real surfaces, although the effects of one group of roughness elements may dominate. As an example, a hypothetical desert surface is offered in Table 1. On this hypothetical surface, loose dust has not been included. This is because the magnitude of shear that loose dust can sustain (before its movement is initiated) is very small compared to the shear transmitted by larger, fixed roughness elements. The hypothetical surface includes roughness elements spanning four orders of magnitude. All are assumed to be spherical. The majority of the surface (80% by area) is covered by fixed, small "sand grains". Nevertheless, the major contributors to roughness are "medium rocks" and "small shrubs", each of which covers only 1% of the surface. It would probably be satisfactory for engineering calculations to use Z_o = 0.622 cm. in Eqn. (8) for this surface (or perhaps a slightly smaller value).

It is worth emphasizing that Z_o bears little direct relation to the physical size of roughness elements. The actual height of the elements is y_R, while Z_o is a characteristic roughness scale that accounts for element size, geometry, and areal coverage.

It may be possible to establish the value of Z_o for a given terrain without a detailed survey like that given in Table 1. An example of this appears in Reference 6. The velocity profile of an atmospheric wind-induced boundary layer was measured (at the GMX area of the Nevada Test Site). The measurements were made using a pitot-static rake of appropriate height. From the velocity profile it was possible to establish a characteristic roughness scale.

Table 1. Distribution of roughness scale Z_o for hypothetical desert surface. Values for Z_o assume spherical roughness elements of diameter y_R and fractional areal coverage f_R.

ROUGHNESS ELEMENT TYPE	y_R (cm)	f_R	Z_o (cm)
Small sand grains	0.02	0.80	0.000495
Large sand grains	0.2	0.16	0.0319
Small rocks	2.0	0.02	0.0280
Medium rocks	10.	0.01	0.0622
Small, dense shrubs	100.	0.01	0.622

While this straightforward procedure is relatively convenient, it is certainly not clear that the roughness scale determined from such measurements can be applied unmodified to the boundary layer of a high-speed, transient flow. It would accordingly seem worthwhile to investigate the possibility for establishing procedures from which the correct scale associated with a high-speed flow could be inferred from the value determined through low-speed wind measurements.

As an alternative, it may prove feasible to establish Z_o for a specific terrain directly from boundary layer profiles measured during an airblast event. The smallest scale at which measurements of this kind would be meaningful is uncertain, but an estimate might be $R_o \gg y_R$, where R_o is a characteristic airblast radius for a surface burst,

$$R_o = \left(\frac{E_o}{2\pi P_1}\right)^{1/3} , \qquad (11)$$

in which E_o is the explosion energy and P_1 is initial ambient pressure.* For example, with $R_o = 20y_R$, $P_1 = 0.1$ MPa, and $y_R = 1$ m, the smallest explosion energy would be $E_o = 5.02 \times 10^9$ J, This suggests that a 0.0024 KT (or 2.4T) surface burst might reasonably suffice for a measurement of Z_o.

---

* At the ground range for which $R = R_o$, the overpressure is $\Delta P \doteq 1.4 P_1$.

SECTION 5
ROUGHNESS SCALING

Finally, it is noted that the characteristic roughness Z_o is a fixed property of the terrain and, perhaps, of the flow regime (Mach and Reynolds numbers). As such, the value of Z_o for a particular surface does not change as the airblast scale is changed; i.e., in this sense Z_o does not "scale". However, for some assessments of airblasts at different scales, it is of interest to hold the global effects of surface roughness constant. In order for the overall effects of roughness to remain unchanged as the airblast scale is changed, it is necessary to allow Z_o to vary. Experimentally, this would require tests to be conducted over surfaces with <u>different</u> Z_o as E_o is changed. It can be shown that the appropriate scaling for <u>equal</u> roughness effects is $Z_{o2}/Z_{o1} = (E_{o2}/E_{o1})^{1/3}$. (That is, "cube-root" scaling is valid.) For example, to simulate the roughness effects of the hypothetical desert surface in Table 1 at 1:27,000 yield scale (1:30 length scale), 1% of the test surface should be covered with fixed spheres, 3.3 cm. in diameter. Experiments at this scale are within the capability of existing confined-flow airblast simulators.

SECTION 6
LIST OF REFERENCES

1. Perry,A. E., et. al., "Rough Wall Turbulent Boundary Layers," J. Fluid Mech. Vol. 37, Part 2, 1969, pp. 383-413.

2. Schlichting, H., Boundary Layer Theory, McGraw-Hill, New York, 1968.

3. Betterman, D., "Contribution A L'Etude de la Conche Limite Turbulante Le Long De Plaques Regueuses," Rapport 65-6, Centre Nat. de la Rech. Sci., Paris France, 1965. Referenced in Cebeci, T. and Smith, A.M.O., Analysis of Turbulent Boundary Layers, New York. Academic Press, 1974, p. 130.

4. Dvorak, F.A., "Calculation of Turbulent Boundary Layers on Rough Surfaces in Pressure Gradient," AIAA J., Vol. 7, No. 9, 1969, p. 1752.

5. Marshall, J.K., "Drag Measurements in Roughness Arrays of Varying Density and Distribution", Agr. Meteorol., Vol. 8, 1971, pp. 269-292.

6. Shinn, J. H., et al, "Observations of Dust Flux in the Surface Boundary Layer for Steady and Nonsteady Cases," in Atmosphere Surface Exchange of Particulate and Gaseous Pollutants (1974), Englemann, R.J., and Sehmel, G.A., Eds., NTIS CONFERENCE-740921, January. 1976, p. 625.

DISTRIBUTION LIST

DNA-TR-88-140

DEPARTMENT OF DEFENSE

AFSOUTH
ATTN: U S DOCUMENTS OFFICER

ARMED FORCES STAFF COLLEGE
ATTN: LIBRARY

ASSISTANT TO THE SECRETARY OF DEFENSE
ATOMIC ENERGY
ATTN: EXECUTIVE ASSISTANT

DEFENSE INTELLIGENCE AGENCY
ATTN: DB
ATTN: G FERRELL
ATTN: R MANN
ATTN: DE(ESTIMATES)
ATTN: DI-5
ATTN: DIA/VPA-2 (FED RES DIV)
2 CYS ATTN: RTS-2B
ATTN: RTS-2C (TECH SVCS & SPT)

DEFENSE NUCLEAR AGENCY
ATTN: DFRA
ATTN: NANF
ATTN: NASF
ATTN: NAWE
ATTN: OPNA
ATTN: OPNS
ATTN: RAEE
4 CYS ATTN: TITL

DEFENSE NUCLEAR AGENCY
ATTN: NVCG

DEFENSE NUCLEAR AGENCY
ATTN: TDTT W SUMMA

DEFENSE TECHNICAL INFO CENTER
2 CYS ATTN: DTIC/FDAB

DIRECTOR NET ASSESSMENTS
ATTN: DOCUMENT CONTROL

INTELLIGENCE CENTER, PACIFIC
ATTN: COMIPAC

JOINT DATA SYSTEM SUPPORT CTR
ATTN: R MASON
ATTN: C-332

JOINT STRAT TGT PLANNING STAFF
2 CYS ATTN: JK (ATTN: DNA REP)
ATTN: STUKMILLER
ATTN: JLT
ATTN: JP
ATTN: JPEP

LAWRENCE LIVERMORE NATIONAL LAB
ATTN: DNA-LL

NATIONAL DEFENSE UNIVERSITY
ATTN: ICAF-ICC
ATTN: NWCO

NATIONAL SECURITY AGENCY
ATTN: CHIEF A GROUP

OFFICE OF THE JOINT CHIEFS OF STAFF
ATTN: ED30(J-3 STRAT OPS DIV)
ATTN: J-3/NUC OPNS BR, STRAT OPNS BR
ATTN: J-5 NUCLEAR & CHEM DIV
3 CYS ATTN: J-5 NUC DIV/STRAT DIV/FP&P DIV
ATTN: J-8/CAD
ATTN: JAD/SFD
ATTN: JAD/SSD

OFFICE OF THE SEC OF DEFENSE
ATTN: NAVAL FORCES
2 CYS ATTN: STRAT PROGRAMS & TNF

STRATEGIC AND THEATER NUCLEAR FORCES
ATTN: DR WOODRUFF

U S EUROPEAN COMMAND
ATTN: ECC3S-CCN

U S EUROPEAN COMMAND
ATTN: ECJ-LW

U S EUROPEAN COMMAND
ATTN: ECJ-2-ITD

U S EUROPEAN COMMAND
ATTN: ECJ-3

U S EUROPEAN COMMAND
ATTN: ECJ2-T

U S EUROPEAN COMMAND
ATTN: ECJ5-N

U S NATIONAL MILITARY REPRESENTATIVE
ATTN: U S DOCUMENTS OFFICER

UNDER SEC OF DEFENSE FOR POLICY
ATTN: DUSP/P
ATTN: USD/P

UNDER SECRETARY OF DEFENSE
ATTN: DEP UND SEC, TAC WARFARE PROG
ATTN: G SEVIN

DEPARTMENT OF THE ARMY

DEP CH OF STAFF FOR OPS & PLANS
ATTN: DAMO-NCN
ATTN: DAMO-NCN
ATTN: DAMO-RQS
ATTN: DAMO-ZXA

DEP CH OF STAFF FOR RSCH DEV & ACQ
ATTN: DAMA-CSM-N

EIGHTH U S ARMY
ATTN: EACJ-PON-NS

HARRY DIAMOND LABORATORIES
ATTN: SLCIS-IM-TL

U S ARMY AIR DEFENSE SCHOOL
ATTN: COMMANDANT

U S ARMY ARMOR SCHOOL
ATTN: ATSB-CTD
ATTN: TECH LIBRARY

U S ARMY BALLISTIC RESEARCH LAB
ATTN: SLCBR-DD-T
ATTN: SLCBR-SS-T

U S ARMY COMB ARMS COMBAT DEV ACTY
ATTN: ATZL-CAP

U S ARMY COMD & GENERAL STAFF COL
ATTN: ACQ LIBRARY DIV
ATTN: ATZL-SWT-A

U S ARMY EUROPE AND SEVENTH ARMY
ATTN: AEAGC

U S ARMY INFANTRY CTR & SCH
ATTN: ATSH-CD-CS

U S ARMY MATERIEL COMMAND
ATTN: AMCCN

U S ARMY MATERIEL SYS ANALYSIS ACTVY
ATTN: AMXSY-CR

U S ARMY MISSILE COMMAND
ATTN: AMSMI-XF

U S ARMY NUCLEAR & CHEMICAL AGENCY
ATTN: MONA-NU

U S ARMY NUCLEAR EFFECTS LABORATORY
ATTN: DR J MEASON

U S ARMY WAR COLLEGE
ATTN: LIBRARY

USA SURVIVABILITY MANAGMENT OFFICE
ATTN: J BRAND

DEPARTMENT OF THE NAVY

MARINE CORPS DEV & EDUCATION COMMAND
ATTN: COMMANDER

NAVAL AIR FORCE
ATTN: COMMANDER

NAVAL AIR FORCE
ATTN: COMMANDER

NAVAL INTELLIGENCE SUPPORT CTR
ATTN: NISC-30

NAVAL OCEAN SYSTEMS CENTER
ATTN: CODE 9642 (TECH LIB)

NAVAL POSTGRADUATE SCHOOL
ATTN: CODE 1424 LIBRARY

NAVAL RESEARCH LABORATORY
ATTN: CODE 1220
ATTN: CODE 2627 (TECH LIB)

NAVAL SEA SYSTEMS COMMAND
ATTN: SEA-09G53 (LIB)
ATTN: SEA-643

NAVAL SURFACE FORCE
ATTN: COMMANDER

NAVAL SURFACE FORCE
ATTN: COMMANDER

NAVAL WEAPONS EVALUATION FACILITY
ATTN: CLASSIFIED LIBRARY

NUCLEAR WEAPONS TNG GROUP, ATLANTIC
ATTN: CODE 221
ATTN: DOCUMENT CONTROL

NUCLEAR WEAPONS TNG GROUP, PACIFIC
ATTN: DOCUMENT CONTROL

OFC OF THE DEP CHIEF OF NAVAL OPS
ATTN: OP 654
ATTN: OP 981

OFFICE OF THE CHIEF OF NAVAL OPNS
ATTN: CNO EXECUTIVE PANEL

OPERATIONAL TEST & EVALUATION FORCE
ATTN: CODE 80

OPERATIONAL TEST & EVALUATION FORCE,
ATTN: INTEL OFFICER

TACTICAL TRAINING GROUP, PACIFIC
ATTN: COMMANDER

TACTICAL WINGS ATLANTIC
ATTN: COMMANDER

THEATER NUCLEAR WARFARE PROGRAM OFC
ATTN: PMS 423

DEPARTMENT OF THE AIR FORCE

AFIA/INKD
ATTN: MAJ COOK

AFIS/INT
ATTN: INT

AIR FORCE SYSTEMS COMMAND
ATTN: DL
ATTN: SD

AIR FORCE WEAPONS LABORATORY
ATTN: SUL

AIR UNIVERSITY LIBRARY
ATTN: AUL-LSE

ASSISTANT CHIEF OF THE AIR FORCE
ATTN: SAF/ALR

DEPUTY CHIEF OF STAFF/AF-RDQM
ATTN: AF/RDQI

DEPUTY CHIEF OF STAFF/XOO
ATTN: AF/XOC

DEPUTY CHIEF OF STAFF/XOX
ATTN: AFXOXFM
ATTN: AFXOXFS

SPACE DIVISION/CWH
ATTN: CWH

STRATEGIC AIR COMMAND
ATTN: NRI/STINFO

STRATEGIC AIR COMMAND
ATTN: STIC (544SIW)

TACTICAL AIR COMMAND
ATTN: TAC/DOA

TACTICAL AIR COMMAND
ATTN: TAC/XPJ

U S AIR FORCES IN EUROPE/DEX
ATTN: USAFE/DEXX

U S AIR FORCES IN EUROPE/DOT
ATTN: USAFE/DOQ

U S AIR FORCES IN EUROPE
ATTN: USAFE/INAT

DEPARTMENT OF ENERGY

LAWRENCE LIVERMORE NATIONAL LAB
ATTN: L-35
ATTN: L-38
ATTN: L-389
ATTN: W HOGAN
ATTN: L-53 TECH INFO DEPT LIB
ATTN: Z DIVISION LIBRARY

LOS ALAMOS NATIONAL LABORATORY
ATTN: D RICHMOND
ATTN: T DOWLER
ATTN: REPORT LIBRARY

SANDIA NATIONAL LABORATORIES
ATTN: TECH LIB 3141
ATTN: R B STRATTON

OTHER GOVERNMENT

CENTRAL INTELLIGENCE AGENCY
ATTN: N10

FEDERAL EMERGENCY MANAGEMENT AGENCY
ATTN: G ORRELL
ATTN: J F JACOBS

U S DEPARTMENT OF STATE
ATTN: PM/TMP

DEPARTMENT OF DEFENSE CONTRACTORS

ADVANCED RESEARCH & APPLICATIONS CORP
ATTN: DOCUMENT CONTROL

BDM CORP
ATTN: C WASAFF
ATTN: J BODE
ATTN: J BRADDOCK
ATTN: R BUCHANAN

BOEING CO
ATTN: H WICKLEIN
ATTN: J W RUSSELL

COMPUTER SCIENCES CORPORATION
ATTN: F EISENBARTH

GRUMMAN DATA SYSTEMS CORPORATION
ATTN: S SHRIER

HORIZONS TECHNOLOGY, INC
ATTN: J PALMER

IIT RESEARCH INSTITUTE
ATTN: DOCUMENTS LIBRARY

INSTITUTE FOR DEFENSE ANALYSES
ATTN: CLASSIFIED LIBRARY
ATTN: J GROTE

JAYCOR
ATTN: R SULLIVAN

KAMAN SCIENCES CORP
ATTN: F SHELTON

KAMAN SCIENCES CORP
ATTN: E CONRAD

KAMAN SCIENCES CORPORATION
ATTN: DASIAC

KAMAN TEMPO
ATTN: DASIAC

MARTIN MARIETTA DENVER AEROSPACE
ATTN: J DONATHAN

ORION RESEARCH INC
ATTN: J E SCHOLZ

PACIFIC-SIERRA RESEARCH CORP
ATTN: H BRODE

PACIFIC-SIERRA RESEARCH CORP
ATTN: D GORMLEY

R & D ASSOCIATES
ATTN: C K B LEE
ATTN: D SIMONS
2 CYS ATTN: DOCUMENT CONTROL

R & D ASSOCIATES
ATTN: C KNOWLES
ATTN: J THOMPSON

R & D ASSOCIATES
ATTN: G GANONG

RAND CORP
ATTN: V JACKSON

RAND CORP
ATTN: B BENNETT

S-CUBED
ATTN: B PYATT
2 CYS ATTN: T PIERCE

SCIENCE APPLICATIONS INTL CORP
ATTN: DOCUMENT CONTROL
ATTN: E SWICK
ATTN: J MARTIN
ATTN: M DRAKE
ATTN: R J BEYSTER

SCIENCE APPLICATIONS INTL CORP
ATTN: J SHANNON
ATTN: L GOURE
ATTN: W LAYSON

SCIENCE APPLICATIONS INTL CORP
ATTN: R CRAVER

TRW INC
ATTN: D SCALLY
ATTN: R BURNETT